HOSTED BY
ELSEVIER
CrossMark
Available online at www.sciencedirect.com
ScienceDirect
Resource-Efficient Technologies 2 (2016) 94–103
www.elsevier.com/locate/reffit

Research paper

ASPEN plus modelling of air–steam gasification of biomass with sorbent enabled CO_2 capture

S. Rupesh *, C. Muraleedharan, P. Arun

Department of Mechanical Engineering, National Institute of Technology Calicut, Calicut, Kerala 673601, India

Received 11 March 2016; received in revised form 6 June 2016; accepted 15 July 2016

Available online 26 July 2016

Abstract

The work deals with the modelling and simulation of carbon dioxide capture in air–steam gasification of saw dust using ASPEN Plus process simulator. The proposed quasi-steady state model incorporates pyrolysis, tar cracking and char conversion using existing experimental data. Prediction accuracy of the developed model is validated by comparing with available experimental results. Effects of CaO addition in air–steam gasification are analysed through key operating parameters such as gasification temperature, equivalence ratio, steam to biomass ratio and gasification efficiency. Maximum H_2 mole fraction of 31.17% is obtained at a temperature of 900 K, equivalence ratio of 0.25, and steam to biomass ratio and sorbent to biomass ratio of unity. The H_2 and CO_2 mole fractions are found to be increased and decreased by 28.10% and 42.6%, respectively, when compared with the corresponding non- sorbent case.

© 2016 Tomsk Polytechnic University. Production and hosting by Elsevier B.V. This is an open access article under the CC BY-NC-ND license (http://creativecommons.org/licenses/by-nc-nd/4.0/).

Keywords: Biomass; Gasification; Modelling; ASPEN Plus; Sorbent

1. Introduction

At present most of the industrial and domestic energy requirements are met through conventional fuels. As these energy sources are depleting at a faster rate with escalating energy demands, future energy may be found from renewable energy sources. Biomass is identified as the largest primary energy source in the world after fossil fuels [1]. Overview of conversion routes for extracting energy from biomass is reported by many researchers [2,3]. Compared to biochemical route, thermo-chemical gasification appears to be more favourable for energy extraction in the form of syngas [4]. Hydrogen, one of the important constituents of syngas, has been receiving more attention as a future energy carrier, being a clean fuel with higher energy density on mass basis. Hydrogen has the potential to be a replacement for conventional fuels if produced from a sustainable source. Syngas can be further enriched in its hydrogen concentration by capturing carbon dioxide using suitable sorbents. Calcium oxide is identified as an economic and effective CO_2 sorbent to enhance hydrogen concentration in syngas through carbonation reaction [5]. Only very few experimental works are reported on biomass gasification with CaO sorbents for CO_2 capture. Simulation modelling based analysis provides valuable insights to supplement experimental studies which are considered to be more realistic. Suitably chosen simulation models can considerably reduce the time and investment involved in exploring the favourable process conditions for sorbent incorporated gasification process. Researchers have successfully used ASPEN Plus simulator, a process modelling software, to simulate processes like fluidised bed combustion [6], coal gasification [7] and integrated coal gasification, and solid oxide fuel cells system [8]. It enables to model and simulate each component of an integrated system separately, using default block settings or by modifying them to perform, in a directed way, using FORTRAN or EXCEL subroutines. A review of gasification models using ASPEN Plus process simulator is given by Puig-Arnavat et al. [9]. Sreejith et al. [10] developed a Gibb's free energy minimisation model for steam gasification of biomass to derive the optimum process condition for gasification. Tar was not considered in the model and char conversion was taken as 100%. Maximum hydrogen concentration of 59.3% was predicted at a temperature of 973 K and steam to biomass ratio of unity. Acharya et al.

* Corresponding author. Department of Mechanical Engineering, National Institute of Technology Calicut, Calicut, Kerala 673601, India. Fax: +91-495 228 7250.

E-mail address: mailtorupeshs@gmail.com (S. Rupesh).

http://dx.doi.org/10.1016/j.reffit.2016.07.002
2405-6537/© 2016 Tomsk Polytechnic University. Production and hosting by Elsevier B.V. This is an open access article under the CC BY-NC-ND license (http://creativecommons.org/licenses/by-nc-nd/4.0/). Peer review under responsibility of Tomsk Polytechnic University.

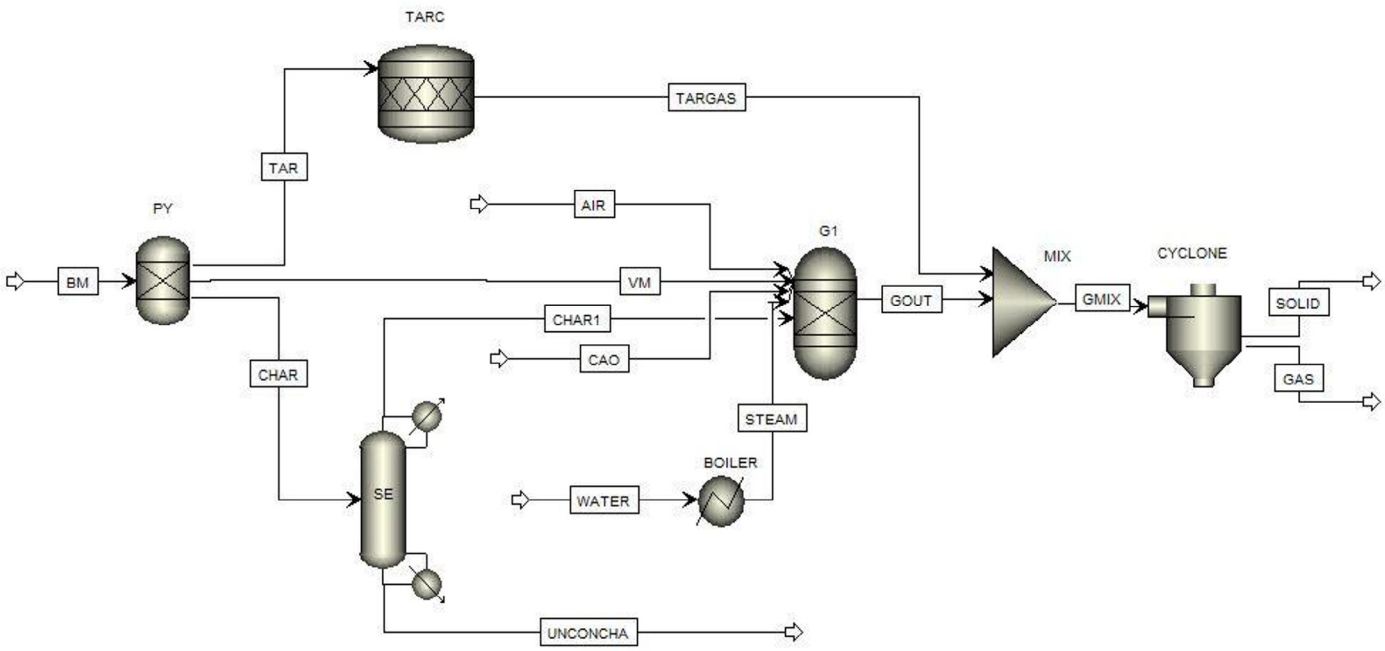

Fig. 1. Process flow sheet for air–steam gasification.

[11] developed a Gibbs free energy based model to simulate sorbent enabled steam gasification of biomass and compared it with their experimental results. Initially the hydrogen yield was found to be over predicted by the model and the deviation from experimental result is reduced by introducing suitable coefficients. Usually the deviation of unmodified equilibrium models is considerable since the entire system will not be in thermodynamic equilibrium. One of the methods to tackle this problem is to model the processes involved in gasification separately. Thus, quasi-steady state models utilise experimentally observed data and correlations to reduce the deviation [12]. Application of ASPEN Plus to simulate biomass air gasification was done by Mansaray et al. [13], neglecting complicated char gasification. Nikoo and Mahinpey [14] conducted a parametric study on air–steam gasification of biomass by integrating the bed hydrodynamics and reaction kinetics in ASPEN Plus. A model to simulate air–steam gasification of biomass in a bubbling fluidised bed for hydrogen and syngas production was developed by Beheshti et al. [15]. They found that higher temperature is favourable for both syngas quality and hydrogen yield, whereas higher equivalence ratio leads to higher carbon conversion, tar reforming, and gas yield at the expense of gas calorific value and cold gas efficiency. Works are not found as reported in sorbent enabled quasi equilibrium modelling of air–steam gasification of biomass using ASPEN Plus. The present work deals with the modelling and simulation of sorbent enhanced air–steam gasification of biomass using ASPEN Plus process simulator.

2. Model development

A non-stoichiometric quasi-steady state model is developed to simulate air–steam gasification of biomass, using ASPEN Plus process simulator. The model will analyse the effect of CaO sorbent for in-situ CO_2 capture. Following are the assumptions made in formulating the model.

- Gasifier is a steady-state system with uniform temperature and pressure throughout.
- Gases except H_2, CO, CO_2, CH_4 and N_2 are considered dilute.
- N_2 is considered as inert in the entire process.
- Biomass is considered to be made up of Carbon, Hydrogen, Oxygen and Nitrogen.
- Steam is supplied at superheated condition of 1 bar and 200 °C.
- Char is assumed as graphitic carbon.
- Catalytic activity of CaO is not considered.

The ASPEN Plus flow sheet of the developed model is shown in Fig. 1. The processes such as pyrolysis, char conversion and tar cracking are incorporated in the model by using FORTRAN subroutines. Amount of char participating in the gasification process and gas species resulted from tar cracking are incorporated in the model based on experimental results [16]. The biomass stream 'BM' is created by inputting the elemental and gross compositions of saw dust obtained from proximate and ultimate analyses, given in Table 1 [17].

Table 1
Proximate and ultimate analyses results.

Proximate analysis (wt. %)		Ultimate analysis (wt. %)	
Volatile matter	76	C	46.46
Fixed carbon	16	H	5.82
Moisture	7	N	0.19
Ash	1	S	0.00
		O	47.51

Pyrolysis of saw dust in the separator 'PY' to char, tar and volatile matter is modelled by using the correlations developed by Gomez-Barea et al. [18]. The tar thus generated is cracked into lighter hydrocarbons in 'TARC'. Fraction of char that undergoes char gasification is considered by adopting the correlation developed by Lim and Lee [19]. The volatile matter 'VM' and char 'CHAR1' are introduced to the gasifier 'G1' where they undergo gasification with the injected steam and air. The syngas is separated from the final gasification product 'GMIX' using a cyclone separator. The description of the blocks used in ASPEN Plus flow sheet is given in Table 2. Initially simulations are carried out without incorporating CaO sorbent.

Gasifier, represented by the R Gibbs reactor 'G1', is an important component in the system where thermochemical gasification process takes place. Gibbs free energy minimisation is the chemical method based on RGibbs reactors function. At thermodynamic equilibrium, total Gibbs free energy of the system is minimum.

Total Gibbs energy of the reacting system is given by

$$G_T = \sum_{i=1}^{N} n_i \mu_i \tag{1}$$

where n and μ are the number of moles and chemical potential of species i, respectively.

Considering ideal gas behaviour for the gases at one atmosphere pressure:

$$\mu_i = \Delta G^0_{f,i} + RT\ln(y_i) \tag{2}$$

Using Eq. (2), Eq. (1) can be rewritten as:

$$G_T = \sum_{i=1}^{N} n_i \Delta G^0_{f,i} + \sum_{i=1}^{N} n_i RT\ln\left(\frac{n_i}{n_{total}}\right) \tag{3}$$

The objective of the problem is to find the value of set of n_i for which total Gibbs free energy of the system is minimum, subjected to the elemental balance constraint given by

$$\sum_{i=1}^{N} a_{ij} n_i = A_j \tag{4}$$

where a_{ij} is the number of atoms of the jth element in a mole of ith species, A_j is the total number of atoms of the jth element in the reaction mixture. By applying Lagrange multiplier method the Gibbs free energy of the system can be minimised using the following expression [20]

$$\frac{\partial L}{\partial n_i} = \Delta G^0_{f,i} + n_i RT\ln\left(\frac{n_i}{n_{tot}}\right) + \sum_{j=1}^{k} \lambda_j a_{ij} = 0 \tag{5}$$

where L is the Lagrange function and λ_j is the Lagrange multiplier. The system of equations contains eight unknowns – five product gas species and three Lagrange multipliers. Out of the eight equations required for the solution, five are obtained from Eq. (5) and the remaining three equations from the elemental balances of carbon, hydrogen and oxygen.

Table 2
Description of blocks in ASPEN Plus flow sheet.

Name in ASPEN Plus	Block ID	Description
Sep	PY	Separator that extracts tar, char and volatile matter from biomass through pyrolysis
RStoic	TARC	Reactor that cracks tar into lighter molecules
Sep2	SE	Separator that enables the extraction of unconverted char from the total char formed
RGibbs	G1	Equilibrium reactor in which the gasification reactions takes place
Mixer	MIX	Mixer which enables the mixing of different streams
Cyclone	CYCLONE	Separates solid particles from the product gas
Heater	BOILER	Boiler to produce steam for gasification

3. Model validation

This section deals with the validation of the developed model by comparing its output with existing experimental results. The prediction accuracy of the model is checked by comparing the model predicted syngas composition with the experimental results from air–steam gasification and sorbent enabled steam and air–steam gasification. Fig. 2 shows the comparison of model results with the experimental results of Loha et al. [21] for air–steam gasification. The deviation of the model results from experimental values is quantified by using statistical parameter RMS (root mean square) error. An RMS error of 2.8 is obtained when eight sets of experimental data are compared with the corresponding model values for product gas composition.

The ability of the model to predict hydrogen concentration in sorbent enabled gasification is also evaluated. Fig. 3 shows the comparison of model predicted hydrogen concentration with the experimental results of Acharya et al. [11] and Mahishi and Goswami [22] for sorbent enabled steam gasification. Applicability of the model for sorbent enabled air–steam gasification is checked by comparing the model predicted hydrogen concentration with that of the experiments done by Xu et al. [23] (Fig. 4). An average deviation of 10.83% is obtained when the simulation results are compared with the experimental data for sorbent enabled gasification.

4. Model application

The validated model is used to analyse the effect of main operating parameters such as gasification temperature, equivalence ratio (ER), steam to biomass ratio (SBR), and sorbent to biomass ratio (SOBR) on product gas composition, lower heating value and gasification efficiency.

Lower heating value of product gas is determined from the product gas composition [24]:

$$LHV_{gas} = 10.79Y_{H_2} + 12.26Y_{CO} + 35.81Y_{CH_4} \tag{6}$$

Gasification efficiency based on hydrogen content in the product gas:

$$\eta_{gas} = \frac{\text{Energy content of } H_2 \text{ in the product gas}}{\text{Energy content in biomass} + \text{Energy content in steam}} \tag{7}$$

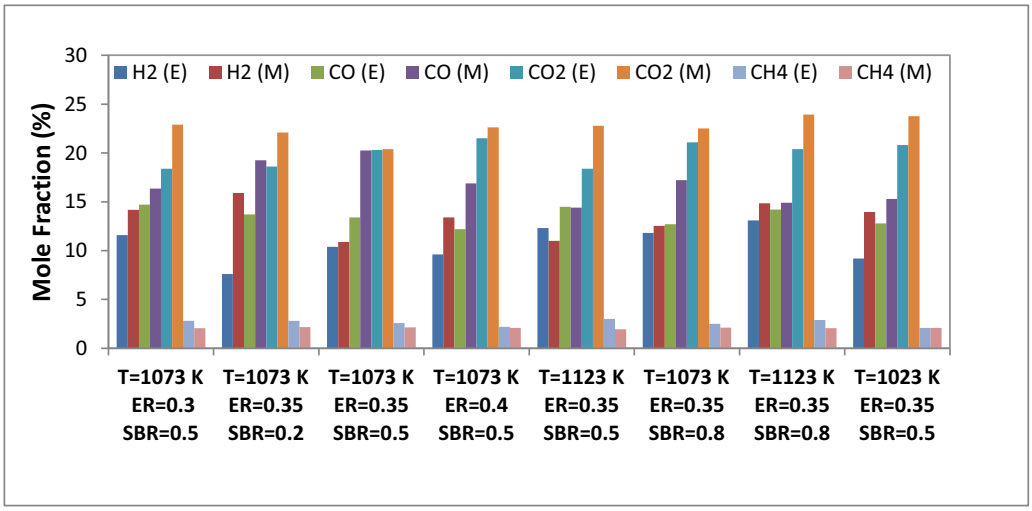

Fig. 2. Comparison between model and experimental (Loha et al. [21]) results. E, experimental result; M, model result.

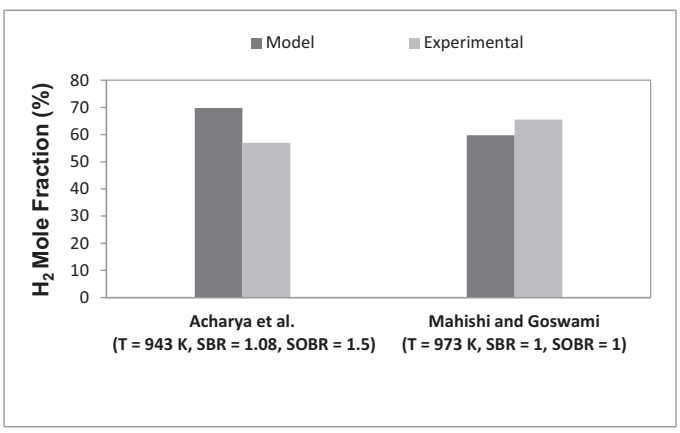

Fig. 3. Comparison between model and experimental (Acharya et al. [11], Mahishi and Goswami [22]) results for hydrogen mole fraction in steam gasification.

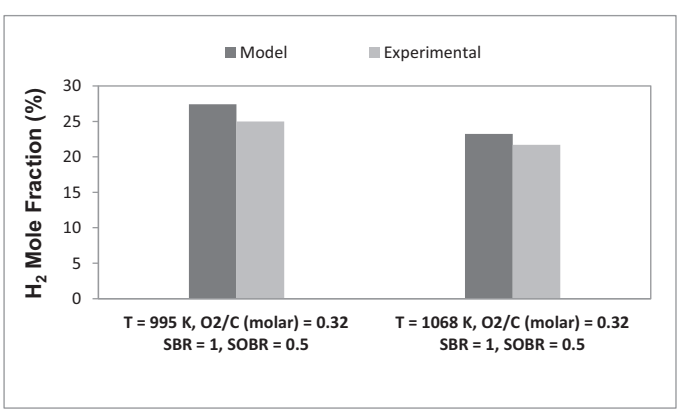

Fig. 4. Comparison between experimental (Xu et al. [23]) and model results for hydrogen mole fraction in air–steam gasification.

5. Results and discussion

5.1. Effect of temperature on product gas composition

The effect of temperature on product gas composition with and without CaO sorbent is depicted through Fig. 5a,b, respectively. In both cases H_2 concentration is found to increase to a maximum value and then decreases with increase in temperature, which is attributed to the reversal of water gas shift reaction. In sorbent enabled gasification, for SOBR of unity, a maximum H_2 concentration of 31.17% is obtained at a gasification temperature of 900 K.

The maximum mole fraction of H_2 is found to be increased by 28.10% when compared with that without CO_2 sorbent. Meanwhile, CO_2 decreases to a minimum value and then increases beyond a temperature of 1000 K in CaO enabled gasification, whereas CO_2 concentration remains almost constant beyond a temperature of 1000 K in gasification without sorbent. This reversal of trend in the variation of CO_2 concentration with temperature, beyond 1000 K, in CaO enabled gasification is due to the reversal of exothermic carbonation reaction (calcination) by Le Châtelier's principle.

Carbonation reaction:

$$CaO(s) + CO_2(g) \rightarrow CaCO_3(s)(\text{exothermic}) \tag{8}$$

Calcination reaction:

$$CaCO_3(s) \rightarrow CaO(s) + CO_2(g)(\text{endothermic}) \tag{9}$$

5.2. Effect of sorbent addition on product gas composition

Fig. 6 shows the effect of mass flow rate of sorbent in product gas composition at a gasification temperature of 1000 K, which corresponds to minimum CO_2 yield. Up to a SOBR of unity, CO_2 is found to decrease with SOBR due to the enhanced carbonation reaction and consequently there is an increase in H_2 and decrease in CO concentrations. This decrease in CO and CO_2, and increase in H_2 with sorbent addition is attributed to the combined effect of carbonation and water gas shift reactions. When sorbent content is increased carbon dioxide in the product gas is captured in the form of $CaCO_3$. This reduction in carbon dioxide reduces its partial pressure in the gas mixture and consequently water gas shift reaction (Eq. (10)) proceeds in the forward direction as per Le Châtelier's principle. At a temperature of 900 K, SBR of 1 and ER of 0.25,

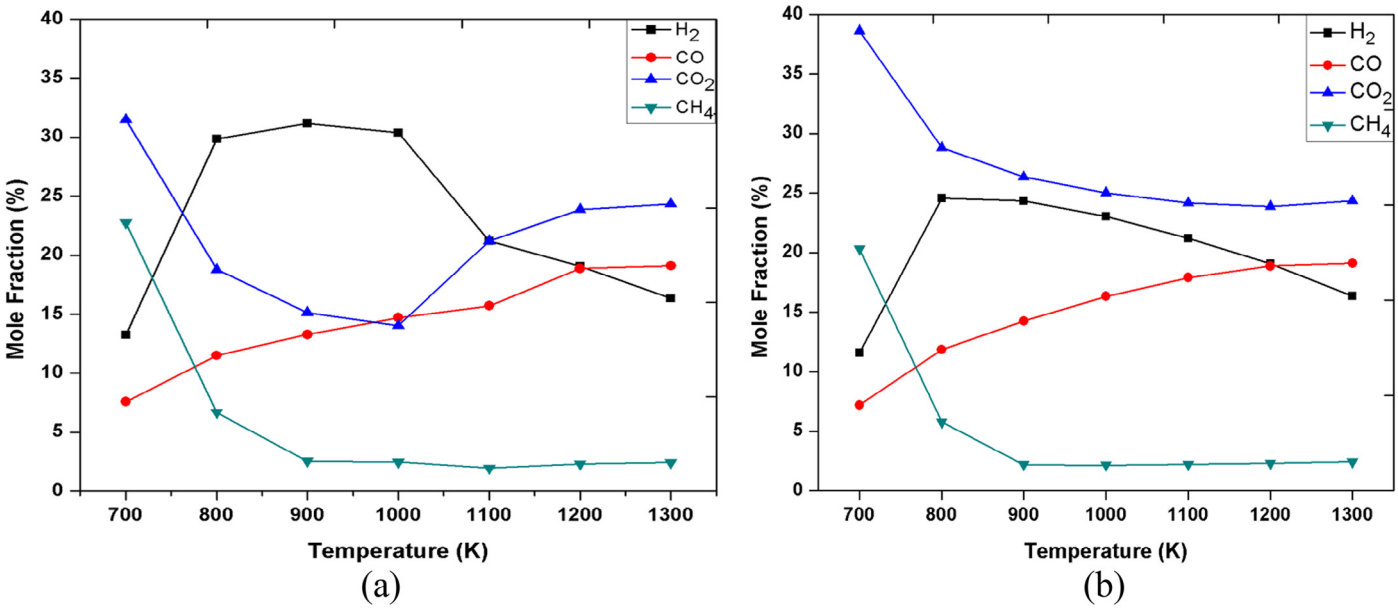

Fig. 5. Effect of temperature on product gas composition. (a) With sorbent (SBR = 1, SOBR = 1, ER = 0.25). (b) Without sorbent (SBR = 1, SOBR = 0, ER = 0.25).

a maximum H_2 mole fraction of 30.50% is obtained at a SOBR of unity.

Water gas shift reaction:

$$CO(g) + H_2O(g) \rightarrow CO_2(g) + H_2(g)(\text{exothermic}) \quad (10)$$

Figs 7a,b compare the effect of steam addition in product gas composition for sorbent enabled gasification with that without sorbent. It is observed that addition of CaO augmented H_2 mole fraction by 32.05% and decreased CO_2 by 43.09% at SBR of unity. The increase in H_2 and CO_2, and decrease in CO concentrations, with SBR, in both cases are due to the effect of water gas shift reaction.

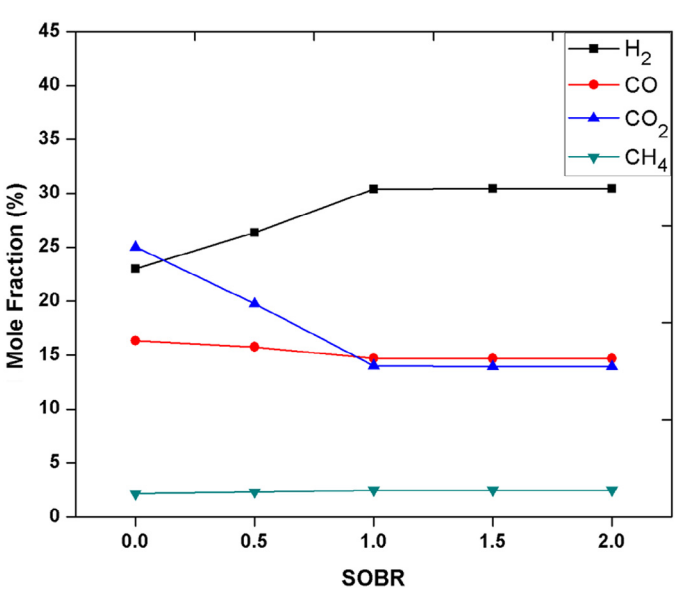

Fig. 6. Effect of SBOR on product gas composition (T = 1000 K, SBR = 1, ER = 0.25).

5.3. Effect of ER on product gas composition

Fig. 8 shows the effect of ER on the mole fraction of product gas constituents with and without CaO. In general, all the gas constituents except CO_2 decrease with ER. This is due to shifting of the process towards combustion at higher ER values. The increase in number of moles of CO_2 with ER is shown in Fig. 9a,b.

Even though the number of moles of CO_2 increases, there is a decrease in CO_2 mole fraction with ER. This is attributed to the higher rate of increase of total number of moles of gas constituents, due to the addition of N_2, compared to the increase in number of moles of CO_2.

5.4. Effect of process parameters on gasification efficiency

Influence of SOBR, ER and SBR on LHV (lower heating value) of product gas is depicted in Fig. 10. Decrease in LHV is found to be insignificant beyond a SOBR of unity. Decrease in LHV of product gas with increase in ER is due to the enhanced combustion at higher air flows. On the other side, SBR has got favourable effect on LHV as steam addition can promote char gasification and water gas shift reactions.

5.5. Effect of gasifying agent on product gas composition

Gasifying agent is another significant parameter which determines product gas composition.

The effect of different gasifying agents on product gas composition in sorbent enabled and normal gasification (without sorbent) is compared in Fig. 11. In both cases H_2 concentration in the product gas is maximum and minimum when steam and air are used as the gasifying agents, respectively. This increased H_2 concentration with steam and air–steam as gasifying agents is mainly due to the effect of water gas shift reaction. Consequently, the concentration of CO in air–steam and steam

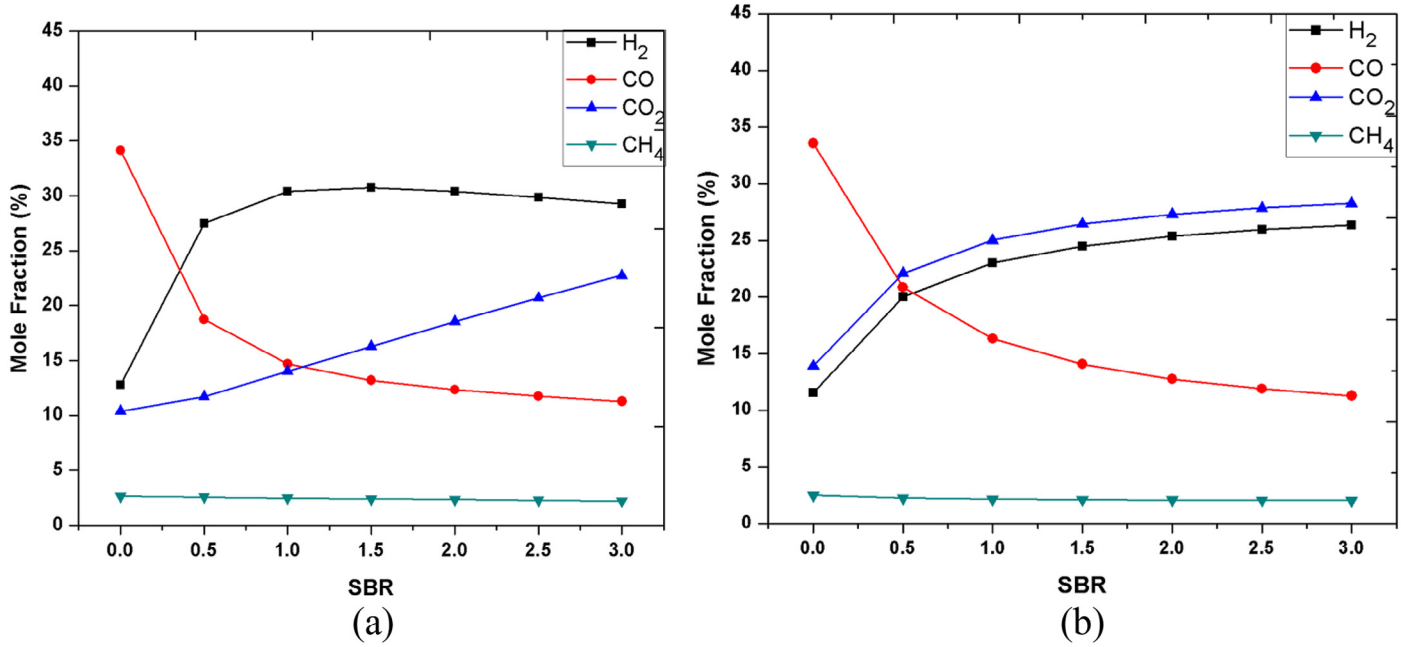

Fig. 7. Effect of SBR on product gas composition. (a) With sorbent (T = 1000 K, SOBR = 1, ER = 0.25). (b) Without sorbent (T = 1000 K, SOBR = 0, ER = 0.25).

gasification is less compared to that of air. It is also observed that as the CO_2 concentration is comparatively less with air as gasifying agent and hence the relative enhancement of H_2 in air gasification is insignificant. For the aforementioned conditions the H_2 concentration is found to be enhanced by 10.47%, 32.05% and 33.08% for air, air–steam and steam gasification, respectively, when compared with the corresponding H_2 concentrations without sorbent. Variation of gas yield [24] with sorbent addition is shown in Fig. 12. The gas yield is found to decrease up to a SOBR of unity as the addition of sorbent captures CO_2 from the product gas.

5.6. *Effect of process parameters on gasification efficiency*

Effect of process parameters on gasification efficiency based on H_2 is shown in Fig. 13.

Efficiency increases with increase in temperature and SBR to a maximum value and then decreases. The decrease in efficiency beyond an SBR of unity is due to the increase in energy

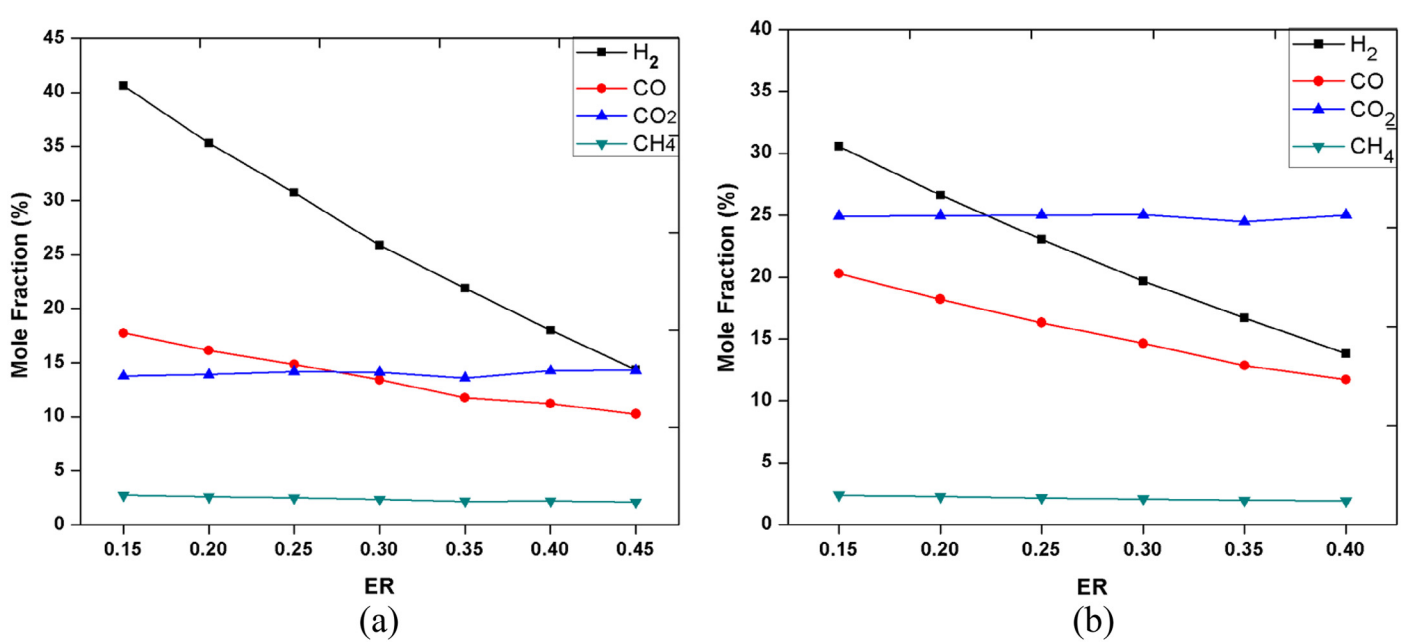

Fig. 8. Effect of ER on product gas composition. (a) With sorbent (T = 1000 K, SOBR = 1, SBR = 1). (b) Without sorbent (T = 1000 K, SOBR = 0, SBR = 1).

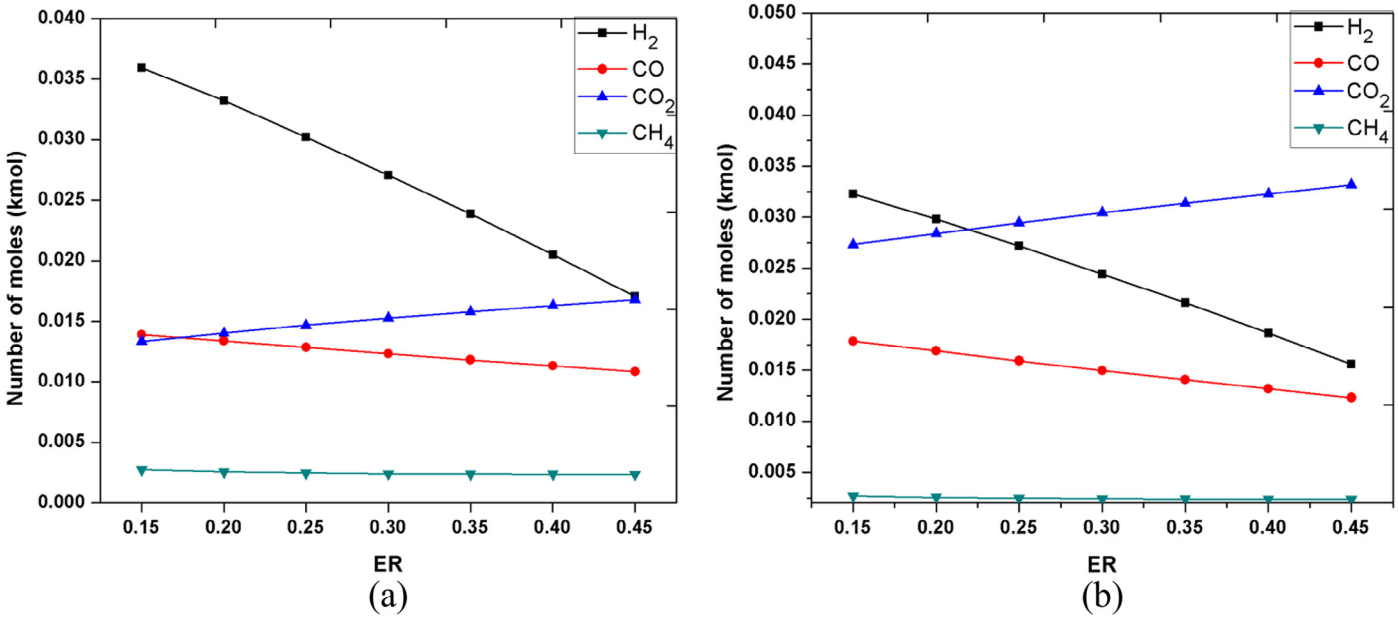

Fig. 9. Effect of ER on number of moles. (a) With sorbent (T = 1000 K, SOBR = 1, SBR = 1). (b) Without sorbent (T = 1000 K, SOBR = 0, SBR = 1).

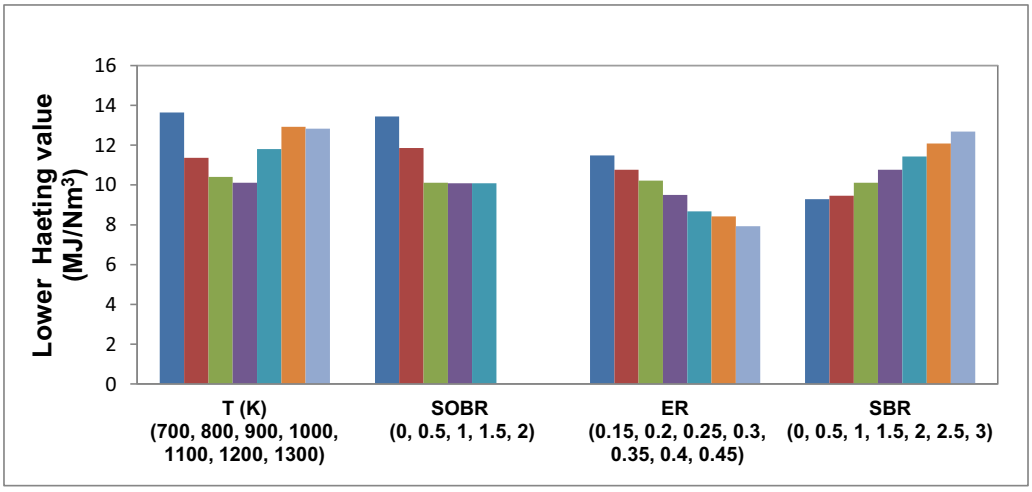

Fig. 10. Effect of T, SOBR, ER and SBR on lower heating value of product gas.

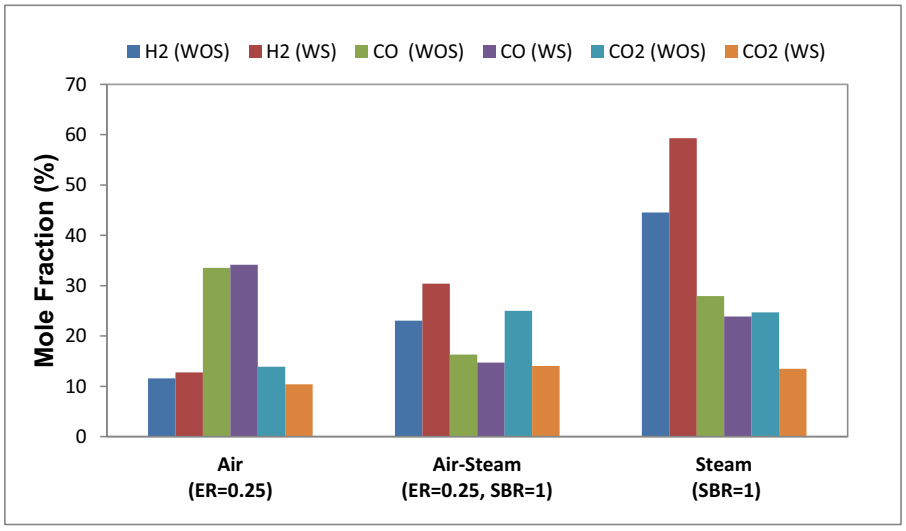

Fig. 11. Effect of gasifying agents in product gas composition (T = 1000 K). WS, with sorbent (SOBR = 1); WOS, without sorbent.

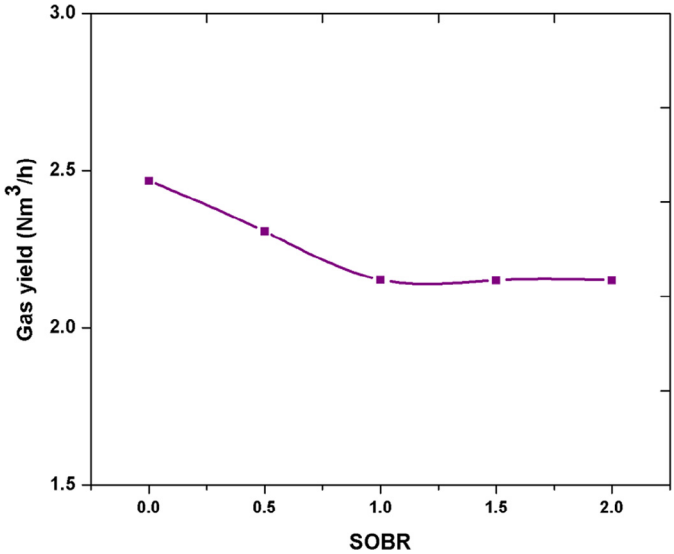

Fig. 12. Effect of SOBR on product gas yield (T = 1000 K, SBR = 1, SOBR = 1, ER = 0.25).

addition in the form of steam. Efficiency is found to increase with sorbent addition up to a SOBR of unity as the H_2 content in the product increases up to a SOBR of unity. The decrease in efficiency with increase in ER is due to the transformation of fuel gas into flue gas at higher ER values.

6. Regression analysis

Simulations are carried out by varying temperature, SBR, SOBR and ER in the ranges from 800 K to 1200 K, 0 to 2.5, 0 to 2.5 and 0.15 to 0.45, respectively, using the developed model. ANOVA is performed, on the developed data, using the statistical tool Design Expert 9 to determine the correlations for the yield of different gas species in terms of main process parameters such as gasification temperature, ER, SOBR and SBR on the yield. The relationship between operating parameters and product gas yield is given in Table 3.

7. Conclusions

A quasi-steady state model was developed in ASPEN Plus process simulator to analyse the effect of key operating parameters on sorbent enabled air–steam gasification of saw dust. Accuracy of the developed model is checked by comparing the model predicted product gas composition with that from literatures. The validated model is used to analyse the effect of gasification temperature, ER, SOBR, and SBR on product gas composition and gasification efficiency. Effect of different gasifying agents on product gas composition was analysed in the presence and absence of CaO sorbent. Regression analysis is performed and correlations for the yield of different syngas constituents were developed. It is inferred from the analysis that, for a SBR and SOBR of unity, a maximum H_2 mole fraction of 31.17% is obtained at 900 K, which is 28.10% higher compared to gasification without sorbent.

Acknowledgement

Authors gratefully acknowledge the financial support provided by Ministry of New and Renewable Energy through R&D project on 'Investigation on bio-hydrogen production by thermo-chemical method in fluidised bed gasifier under catalytic support and its utilisation' (No. 103/181/2010-NT).

Table 3
Regression equations for product yield.

Species (% vol.)	Regression equation	Adj. R^2 (%)	R^2 (%)
H_2	$-140.02314 + 0.28755*T + 4.44918*SOBR + 78.86051*ER + 34.75985*SBR - 4.23602E-3*T*SOBR - 0.098546*T*ER - 9.55340E-3*T*SBR + 2.04336*SOBR*SBR - 31.26554*ER*SBR - 1.29577E-004*T^2 - 5.44316*SBR^2$	88.2	88.54
CO	$-18.01030 + 0.12293*T - 56.02196*ER - 35.62464*SBR - 0.067121*T*ER + 47.69225*ER*SBR - 4.47715E-5*T^2 + 59.14027*ER^2 + 7.38489*SBR^2$	97.92	97.96
CO_2	$175.53217 - 0.31958*T - 25.33447*SOBR - 12.64238*ER + 19.98347*SBR + 0.020091*T*SOBR + 0.041292*T*ER - 24.76819*ER*SBR + 1.49544E-4*T^2 - 4.27176*SBR^2$	88.86	89.13
CH_4	$188.14061 - 0.33123*T + 6.31783*SOBR - 71.84718*ER - 8.76893*SBR - 5.04188E-3*T*SOBR + 0.059646*T*ER + 6.71989E-3*T*SBR - 0.76362*SOBR*SBR + 4.44864*ER*SBR + 1.47715E-4*T^2$	91.01	91.25

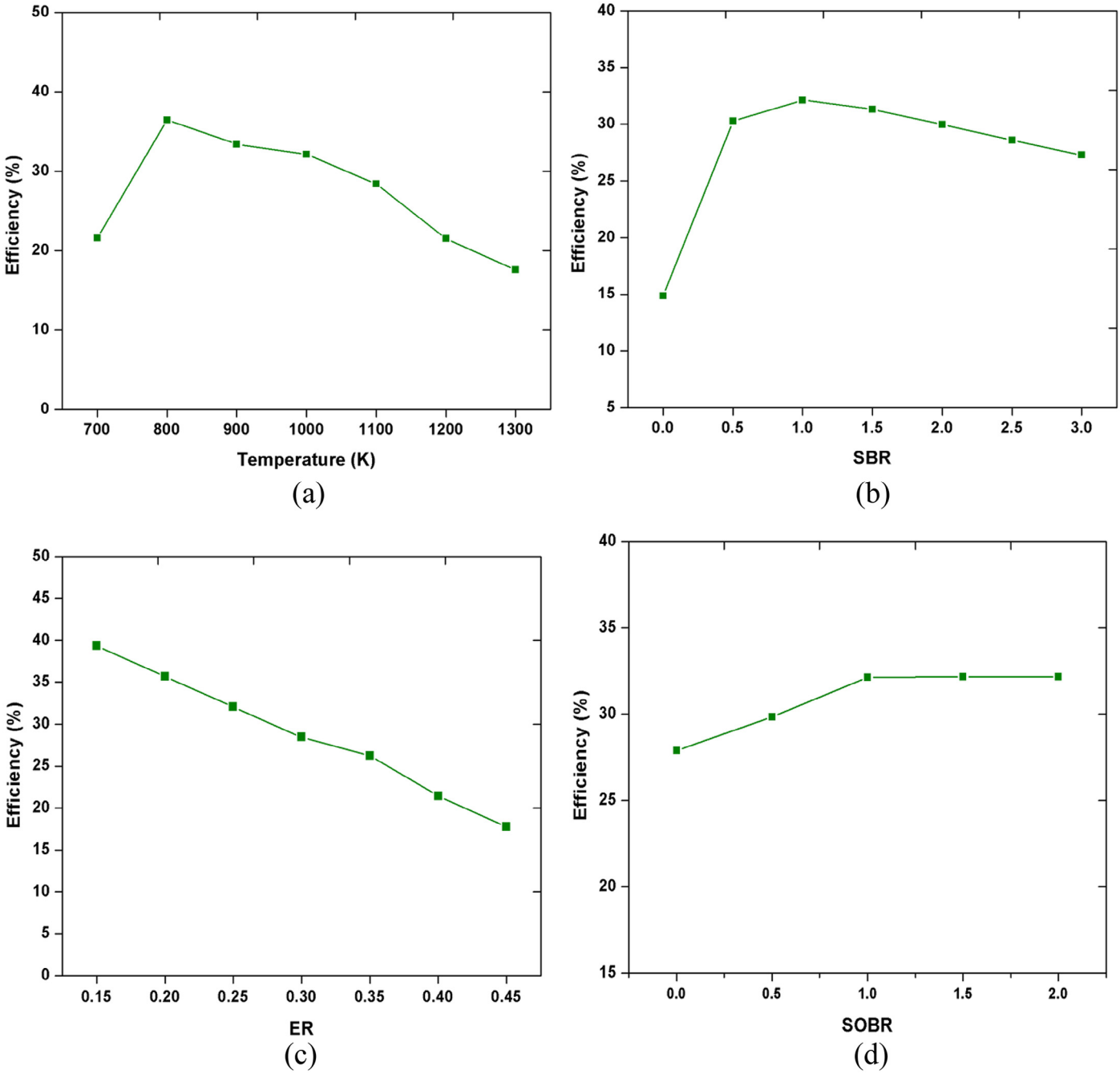

Fig. 13. Effect of process parameters on efficiency. (a) Temperature (SBR = 1, SOBR = 1, ER = 0.25). (b) SBR (T = 1000 K, SOBR = 1, ER = 0.25). (c) ER (T = 1000 K, SOBR = 1, SBR = 1). (d) SOBR (T = 1000 K, SBR = 1, ER = 0.25).

References

[1] J. Werther, M. Saenger, E.U. Hartge, T. Ogada, Z. Siagi, Combustion of agricultural residues, Prog. Energy Combust. Sci. 26 (2000) 1–27, doi:10.1016/S0360-1285(99)00005-2.

[2] I. Dincer, Green methods for hydrogen production, Int. J. Hydrogen Energy 37 (2012) 1954–1971, doi:10.1016/j.ijhydene.2011.03.173.

[3] P. Basu, Biomass gasification and pyrolysis handbook, 2010. http://dx.doi.org/10.1016/B978-0-12-374988-8.00001-5.

[4] S. Sharma, P.N. Sheth, Air–steam biomass gasification: experiments, modeling and simulation, Energy Convers. Manag. 110 (2016) 307–318, doi:10.1016/j.enconman.2015.12.030.

[5] N.H. Florin, A.T. Harris, Enhanced hydrogen production from biomass with in situ carbon dioxide capture using calcium oxide sorbents, Chem. Eng. Sci. 63 (2008) 287–316, doi:10.1016/j.ces.2007.09.011.

[6] P.L. Douglas, B.E. Young, Modelling and simulation of an AFBC steam heating plant using ASPEN/SP, Fuel 70 (1991) 145–154, doi:10.1016/0016-2361(91)90145-Z.

[7] H.M. Yan, V. Rudolph, Modelling a compartmented fluidised bed coal gasifier process using Aspen Plus, Chem. Eng. Commun. 183 (2000) 1–38, doi:10.1080/00986440008960499.

[8] S. Chen, N. Lior, W. Xiang, Coal gasification integration with solid oxide fuel cell and chemical looping combustion for high-efficiency power generation with inherent CO2 capture, Appl. Energy 146 (2015) 298–312, doi:10.1016/j.apenergy.2015.01.100.

[9] M. Puig-Arnavat, J.C. Bruno, A. Coronas, Review and analysis of biomass gasification models, Renew. Sustain. Energy Rev. 14 (2010) 2841–2851, doi:10.1016/j.rser.2010.07.030.

[10] C.C. Sreejith, C. Muraleedharan, P. Arun, Performance prediction of steam gasification of wood using an ASPEN PLUS thermodynamic equilibrium model, Int. J. Sustain, Energy 33 (2013) 416–434, doi:10.1080/14786451.2012.755977.

[11] B. Acharya, A. Dutta, P. Basu, An investigation into steam gasification of biomass for hydrogen enriched gas production in presence of CaO, Int. J. Hydrogen Energy 35 (2010) 1582–1589, doi:10.1016/j.ijhydene.2009.11.109.

[12] S. Rupesh, C. Muraleedharan, P. Arun, A comparative study on gaseous fuel generation capability of biomass materials by thermo-chemical gasification using stoichiometric quasi-steady-state model, Int. J. Energy Environ. Eng. 6 (2015) 375–384, doi:10.1007/s40095-015-0182-0.

[13] K. Mansaray, A.M. Al-Taweel, A.E. Ghaly, V.I. Ugursal, Mathematical modeling of a fluidized bed rice husk gasifier: part I-model development, Energ. Sources 22 (2000) 83–98, doi:10.1080/00908310050014243.

[14] M.B. Nikoo, N. Mahinpey, Simulation of biomass gasification in fluidized bed reactor using ASPEN PLUS, Biomass Bioenergy 32 (2008) 1245–1254, doi:10.1016/j.biombioe.2008.02.020.

[15] S.M. Beheshti, H. Ghassemi, R. Shahsavan-Markadeh, Process simulation of biomass gasification in a bubbling fluidized bed reactor, Energy Convers. Manag. 94 (2015) 345–352, doi:10.1016/j.enconman.2015.01.060.

[16] M.L. Boroson, J.B. Howard, J.P. Longwell, W.A. Peters, Product yields and kinetics from the vapor phase cracking of wood pyrolysis tars, AIChE J. 35 (1989) 120–128, doi:10.1002/aic.690350113.

[17] O. Mohan, S. Rupesh, C. Muraleedharan, P. Arun, Design of fluidized bed reactor for conversion of biomass energy into concentrated gaseous fuel, IEEE International Conference on Signal Processing, Informatics, Communication and Energy Systems (IEEE SPICES) February, 2015, NIT Calicut, 2-6.

[18] A. Gomez-Barea, S. Nilsson, F.V. Barrero, M. Campoy, Devolatilization of wood and wastes in fluidized bed, Fuel Process. Technol. 91 (2010) 1624–1633, doi:10.1016/j.fuproc.2010.06.011.

[19] Y. Lim, U. Lee, Quasi-equilibrium thermodynamic model with empirical equations for air–steam biomass gasification in fluidized-beds, Fuel Process. Technol. 128 (2014) 199–210, doi:10.1016/j.fuproc.2014.07.017.

[20] S. Shabbar, I. Janajreh, Thermodynamic equilibrium analysis of coal gasification using Gibbs energy minimization method, Energy Convers. Manag. 65 (2013) 755–763, doi:10.1016/j.enconman.2012.02.032.

[21] C. Loha, H. Chattopadhyay, P.K. Chatterjee, Thermodynamic analysis of hydrogen rich synthetic gas generation from fluidized bed gasification of rice husk, Energy 36 (2011) 4063–4071, doi:10.1016/j.energy.2011.04.042.

[22] M.R. Mahishi, D.Y. Goswami, An experimental study of hydrogen production by gasification of biomass in the presence of a CO2 sorbent, Int. J. Hydrogen Energy 32 (2007) 2803–2808, doi:10.1016/j.ijhydene.2007.03.030.

[23] G. Xu, T. Murakami, T. Suda, S. Kusama, T. Fujimori, Distinctive effects of CaO additive on atmospheric gasification of biomass at different temperatures, Ind. Eng. Chem. Res. 44 (2005) 5864–5868, doi:10.1021/ie050432o.

[24] S. Kaewluan, S. Pipatmanomai, Potential of synthesis gas production from rubber wood chip gasification in a bubbling fluidised bed gasifier, Energy Convers. Manag. 52 (2011) 75–84, doi:10.1016/j.enconman.2010.06.044.